Nighttime characterization of AOD and water vapor using lunar photometry. Synergies with Lidar technique

A. Barreto[1,2], E. Cuevas[1], A. Mortier[3,4], P. Goloub[3], T. Podvin[3], L. Blarel[3], V. Choliy[5], and Y. Hernández[1]

[1]Izaña Atmospheric Research Center, Meteorological State Agency of Spain (AEMET), Spain
[2]Cimel Electronique, Paris, France
[3]Laboratoire d' Optique Atmosphérique, Lille, France
[4]Chinese Academy of Sciences, Beijing, China
[5]Astronomy and Space Physics Department, Kyiv National Taras Shevchenko University, Kyiv, Ukraine

Corresponding author. *E-mail*: africabv@gmail.com

Abstract

The combined lidar and sun-photometer system is currently implemented and successfully checked to derive vertically-resolved aerosol information. This paper presents the enhancement of the synergy lidar/photometer at nighttime using the lunar-photometer CE-318U and the lidar CE-370. We have firstly assessed the Aerosol Optical Depth (AOD) and Precipitable Water Vapor (PWV) obtained from the new lunar-photometer CE-318U using daytime data extracted from AErosol RObotic NETwork (AERONET). The comparative study showed AOD and PWV discrepancies within the expected precision for daytime conditions (up to $\pm$ 0.02 for AOD and $\sim$ 10% for PWV) under high moon illumination conditions (up to $\sim$ 85%), with higher inaccuracies found as illumination becomes lower. This is attributed to uncertainties on the ROLO model as well as the expected decrease in signal-to-noise ratio.

The synergetic retrieval of AOD at nighttime using the combined CE-318U and the lidar CE-370 demonstrated the improvement in the extinction vertical profile at nighttime if the inversion is constrained using AOD from lunar-photometer CE-318U instead of the daytime lidar ratio (S_a) value. Our calculations showed that the assumption of S_a for lidar inversion would result in an underestimation up to 40% at nighttime as a consequence of possible changes in the relative humidity not considered if only daytime information is included.

Finally, we introduced briefly the new photometer CE-318T, recently developed to perform a complete cycle of daytime and nighttime measurements. Its new features allow us to improve significantly the accuracy of these photometric measurements as well as to reduce the complexities inherent to nocturnal calibration.

1 INTRODUCTION

The amount of solar energy that incides on the Earth's surface is the major component governing the surface energy balance, determining the Earth's climate. On one hand, aerosols are known to play an important role in this energy balance by scattering and absorbing the solar radiation as well as through their impact on cloud formation. However, important uncertainties still exist in our current understanding of the complex influence of aerosols on climate forcing. Therefore, aerosols have been identified as one of the greatest sources of uncertainty in the estimation of the future climate change scenario. On the other hand, atmospheric water vapor is the most important atmospheric greenhouse gas, and its phases changes involve exchanges of latent heat energy that affects the vertical stability of the atmosphere and the energy balance of the global climate system.

In this sense, accurate knowledge of spatial and temporal observations of aerosol and water vapor concentration are relevant nowadays. This information can be obtained in various ways. The ground-based aerosol and water vapor monitoring systems, providing a validation tool for global satellite products.

The role of sun photometers in the Aerosol Optical Depth (AOD) records spanned most of the 20th century (Holben et al., 2001), being the globally distributed AErosol RObotic NETwork (AERONET) one of the most important attempt for long-term monitoring of atmospheric aerosols and water vapor. This is a global sun photometer network that offers standarization for ground-based regional to global scale aerosol monitoring using the automatic low maintenance radiometers CE-318, in addition to real time date reception accesible for the scientific community (Holben et al., 2001). However, in spite of the high spectral resolution provided by this sun photometers two important disadvantages have been detected:

1. The information extracted using sun photometers are limited to the light period, preventing the existence of aerosol and water vapor monitoring with the required temporal resolution for climate studies. Since very limited energy exists at night, signals used to be far below the sensitivity of the conventional sun photometers. However, in Barreto et al. (2013a,b) was presented a new photometer prototype (CE-318U) to perform lunar measurements to characterize aerosols and precipitable water vapor at nighttime. Higher signal-to-noise ratios enable this instrument suitable to derive, in combination with the current AERONET CE-318, a continuous sequence of diurnal aerosol and water vapor concentrations.

2. The columnar properties inferred using this technique are an important limitation for accounting the vertical humidity profile as well as the indirect effect of aerosols, like their influence on cloud formation (Lopatin et al., 2013), or their direct effect through absorption or backscattering at elevated layers.

The use of active remote measurements by means of advanced ground-based lidars systems permits determining vertical profiles of aerosol optical properties and estimates some microphysical properties, but the relatively limited information from the altitude profiles of the spectral backscattering needs to introduce some physical or mathematical constrains in the inversion algorithm. These assumptions usually rely on aerosol columnar properties and, in combination with known boundary conditions, allow the quantitative interpretation of the lidar backscatter signal (Lopatin et al., 2013). Due to all these reasons, the combined lidar-photometer observations are been currently implemented and successfully checked (Fernald, 1984; Klett, 1985; Cuesta et al., 2008). An example in the literature is the numerical tool LIRIC (LIdar/Radiometer Inversion Code), developed by Chaikovsky et al. (2012) to retrieve vertically resolved aerosol microphysical properties by combining backscattering coefficient measurements from the European Aerosol Research LIdar NETwork (EARLINET) and sun photometer observations from AERONET. More recently, the GARRLiC (Generalized Aerosol Retrieval from Radiometer and lidar Combined data) method was introduced by Lopatin et al. (2013). In spite that both methods use AERONET AOD's, and both approaches for treating lidar data (GARRLiC and LIRIC) are based in the same principles, in the GARRLiC method, the size intervals of the modes may overlap and the size-independent complex refractive index may be different for each aerosol mode (Perrone et al., 2014).

In this work we showed firstly the assessment of the nighttime aerosol and precipitable water vapor (PWV) characterization retrieved by means of the lunar-photometer CE-318U. This prototype was presented in Barreto et al. (2013a,b) who demonstrate the ability of this new device to perform nocturnal measurements with similar accuracies than those associated to daytime. In this study we extended this assessment to a wider range of moon illumination conditions. In the second part of this paper we presented the advantage of a combined system of lidar and moon photometer to enhance the aerosol characterization during nighttime using the CE-318U. Finally, we introduced a brief description and preliminary results of the new photometer CE-318T, recently developed as a combination of the features of the extensively used CE-318 with the ability to perform nocturnal measurements of the CE-318U, capable of taking measurement during daytime and nighttime.

2 INSTRUMENTATION

2.1 The Cimel CE-318U

The Cimel CE-318U lunar-photometer was developed by the French company Cimel Electronique and presented in Barreto et al. (2013a,b) as an attractive option to expand the aerosol characterization at nighttime and to enhance the operational capability of the actual aerosol networks, like AERONET. Among the features of this new instrument are:

- A continuous correction of sun movements between trackings by means of micro-steps, which improves the pointing accuracy.
- A new digital 4-quadrant tracker, which increases the tracking reliability, speed and accuracy.

All these features imply that the CE-318U is characterized by a higher signal-to-noise ratio than the usual CE-318 and therefore make possible the detection of the limited energy at nighttime. In adittion, this lunar-photometer might be used not only to implement aerosol databases covering both day and night periods, but also to improve the accuracy of a particularly important atmospheric gas as the water vapor retrieval (Barreto et al., 2013b).

The CE-318U performs direct moon measurements at an approximate field of view of 1.29° at ten nominal wavelengths of 1640, 1020, 937, 870, 675, 500, 440, 380 and 340 nm, detected using a silicon photodiode detector, as well as one measurement more at 1020 nm using an InGaAs detector. Due to the low signal in the UV channels at night, this information is not useful for AOD or PWV calculation at night.

As in the previous version, the CE-318U takes a sequence of three measurements (triplets) every 30 seconds at each wavelength. The triplet value is defined as the maximum minus minimum divided by the mean value of these three consecutive measurements. At this moment, the triplet information is used to detect and screen clouds as well as to check the instrument's stability until a new operative cloud screening will be applied.

2.2 Lidar system

The CE-370 Lidar, also developed by Cimel Electronique, is a biaxial micro-Lidar which, through its relative simplicity, provides continuous (24/7) elastic backscattered profiles at 532 nm. These profiles extend from 150 m to 30 km with a vertical resolution of 15 m. The low power beam (around 100 mW) is balanced by the high frequency Laser emission (4.7 kHz), which ensures satisfying Signal to Noise Ratio up to 12 km daytime under typical AOD conditions of 0.2-0.25 and for an acquisition time of 10 minutes. A more detailed description of the device is presented by Pelon et al. (2008) and Mortier et al. (2012).

The automatism of the device affords continuous profiles, daytime and nighttime. This characteristic permits the study of specific aerosol events, like dust and biomass burning particles transort (Pelon et al., 2008), volcanic aerosols (Mortier et al., 2012) as well as, if it is used with an appropriate processing system, the study of long term aerosol vertical distributions (Leon et al., 2009; Mortier, 2013).

3 LUNAR PHOTOMETRY USING CE-318U

3.1 Instrument's calibration

According to Barreto et al. (2013a), calibration under nighttime conditions can be attained by transference from a calibrated instrument (using the ratio of moon measurements) but the absolute calibration can not be performed using the Langley-Bouguer technique. The reason is that, unlike the sun, the moon is a highly variable source which changes continuously with the lunar viewing geometry. Thus, Barreto

Table 1: Coefficients a and b obtained for CE-318T.

a	0.5870
b	0.5422

et al. (2013a) developed the Lunar Langley Method that modify the usual Langley technique to be applied under variable illumination conditions. In this method the calibration coefficient can be expressed as,

$$V_{0,\lambda} = I_{0,\lambda} \cdot \kappa_\lambda \tag{1}$$

where $I_{0,\lambda}$ is the extraterrestrial irradiance in a certain channel with a central wavelength at λ, and κ_λ is the instrument calibration constant, which depends on the instrument features. $I_{0,\lambda}$ is calculated using the implementation of the ROLO (RObotic Lunar Observatory) model presented in Kieffer and Stone (2005). This empirical model provides the exo-atmospheric lunar irradiance with relatively high precision ($\sim 1\%$). It requires several astronomical parameters, as lunar phase, sun-moon distance, as well as the selenographic latitude and longitude of the observer and the sun. κ_λ constant strictly accounts for the instrument's photometric responsivity and any residual systematic offset difference between ROLO predicted $I_{0,\lambda}$ and the actual exoatmospheric irradiance.

In this work the absolute calibration was carried out at Izaña Atmospheric Research Center (IARC), at an altitude of 2363 m a.s.l. We computed the spectral calibration constant κ_λ for nighttime using the Lunar Langley Method from the average of 6 different nights, all of them affected by low and quite stable aerosol loads.

3.2 PWV determination

The Beer-Lambert-Bouguer Law must be modified in those spectral regions affected by strong spectral variation of molecular absorption. We do this taking into account the water vapor transmittance: $T_{w,\lambda}$ (Schmid et al., 1996). As Bruegge et al. (1992); Halthore et al. (1997) showed, $T_{w,\lambda}$ present a exponential dependence with PWV:

$$T_{w,\lambda} = exp(-a(m_w(\theta) \cdot PWV)^b) \tag{2}$$

As shown by Barreto et al. (2013b), the "a" and "b" constants can be determined by fitting the simulated $T_{w,\lambda}$ by a radiative transfer model for an specific filter function versus the PWV. Hence, PWV is obtained using the following expression:

$$PWV = \frac{1}{m_w} \cdot \{\frac{1}{a} \cdot [ln(\frac{I_{0,\lambda}}{V_\lambda}) + ln(\kappa_\lambda) - m_R \cdot \tau_{R,\lambda} - m_a \cdot \tau_{a,\lambda}]\}^{\frac{1}{b}} \tag{3}$$

In this equation, m_w represents the water vapor optical mass, m_R is the Rayleigh optical mass and $\tau_{R,\lambda}$ is the Rayleigh optical depth within water vapor absorption band. $I_{0,\lambda}$ is obtained from the ROLO lunar irradiance model, τ_a in this spectral region is obtained by extrapolation of τ_a at 870 and 440 nm, and "a" and "b" constants are obtained by simulation of water vapor transmittances using the radiative code MODTRAN 4.0 (table 1).

4 METHODOLOGY FOR LIDAR PROCESSING AND SYNERGY WITH PHOTOMETER DATA

The basis of the methodology for lidar processing involves a range corrected attenuated backscattering signal with the form (Mortier et al., 2012):

$$P(z) = K \cdot (\beta_a(z) + \beta_m(z)) \cdot exp(-2 \cdot \int_{z_{min}}^{z} (\sigma_{a,ext}(z') + \sigma_m(z'))dz') \quad (4)$$

where z denotes the distance to the scattering object, β_a and β_m are the backscattering coefficients for aerosols and molecules, respectively, $\sigma_{a,ext}$ and σ_m are the exctinction coefficient for aerosols and molecules, respectively, and K is a purelly instrumental parameter. The estimation of K can leads to important uncertainties and it is a critical point in the retrieval algorithm. More information about K calculation can be obtained in Mortier et al. (2012).

Since the terms β_m and σ_m can be easily determined, the particle backscatter and exctinction are unknown values. Thus, the equation 4 is from mathematical point of view an ill-posed problem. To solve this problem the exctinction-to-backscatter coefficient ratio or Lidar Ratio, S_a, is defined as follows,

$$S_a = \frac{\sigma_{a,ext}}{\beta_a} \quad (5)$$

Hence, Eq. 4 can be written as,

$$P(z) = K \cdot (\frac{\sigma_{a,ext}(z)}{S_a} + \beta_m(z)) + exp(-2 \cdot \int_{z_{min}}^{z} (\sigma_{a,ext}(z') + \sigma_m(z'))dz') \quad (6)$$

After calibration and background correction, lidar inversion is constrained using accurate CE-318 AOD and therefore retrieval of $\sigma_{a,ext}$ profile and effective S_a can be performed during daytime. We take the advantage of nocturnal CE-318U AOD's to derive the $\sigma_{a,ext}(z)$ during nighttime, in spite of using the prescribed average S_a as is commonly done, but this assumption could result in large errors if the nature or state of particles changes.

The synergy between lidar and sun photometer can also be done with their respective inversion products. The extinction coefficient derived from the previously described method can be written as below,

$$\sigma_{a,ext}(z) = \int_{r_{min}}^{r_{max}} \pi r^2 Q_{ext}(r, m(z)) \cdot n(r, z)dr \quad (7)$$

where Q_{ext} is the extinction efficiency factor at 532 nm, m the complex refractive index at a respective wavelength and $n(r, z)$ the number size distribution defined for particles radius r between r_{min} and r_{max}. The columnar refractive index, m, is derived by sun-photometer (daytime) inversions, as well as $n(r)$, which is linked to the volume size distribution directly given by AERONET. The calculation of Q_{ext} is computed in case of spheric particles with Mie theory.

By splitting the number size distribution into $n(r) = n_0 \cdot n_1(r)$, where n_1 is the normalized size distribution and n_0 its amplitude, and by assuming a density of particles ρ, one can assess the aerosols mass concentration as follows,

$$[aer](z) = \frac{4}{3}\sigma_{a,ext}(z) \int_{r_{min}}^{r_{max}} \frac{\rho(r)n_1(r)r^3}{\int_{r_{min}}^{r_{max}} Q_{ext(m,r)}n_1(r)r^2dr}dr \quad (8)$$

An assessment of different errors on the mass concentration caluclation provided by this method is given by Mortier et al. (2012).

Since 1994, the LOA conducts continuous passive remote sensing observations with a CE-318 sun-photometer at Mbour (West Africa). This site if of particular interest for dust observations close to desertic sources. An automatic process has been developped at LOA to compute the whole database. A quality check, including clouds detection, was first applied, before to process extinction profiles with the inversion constrained by the AOD measured by the sun-photometer, as it was previously described. In order to improve the accuracy of the vertical extinction profiles at nighttime, a lunar-photometer (CE-318U) operates since 2013 in Mbour observation site. This instrument will increases significantly the number of daily AOD measurement and therefore the accuracy of the respective lidar constrained inversions.

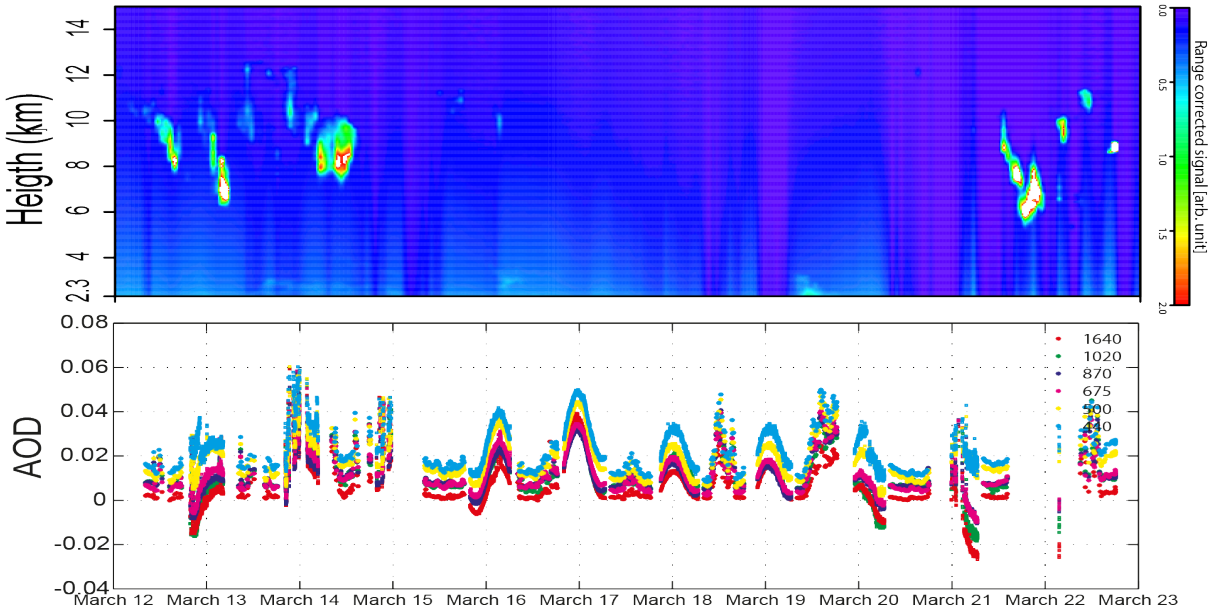

Figure 1: AOD evolution during 10 different days and 9 different nights in March, 2014 using CE-318T data at Izaña Observatory in the upper panel, and corrected backscatter cross-sections from the Izaña altitude extracted from Santa Cruz station MPL in the lower panel.

5 RESULTS AND DISCUSSION

5.1 Aerosol Optical Depth

We present in Fig. 1 the daytime and nighttime AOD evolution for a sequence of 10 different days extracted from AERONET and 9 different nights from CE-318U in March, 2014. We also show the corrected backscatter cross-sections from Izaña altitude on measured using a micropulse Lidar (MPL) sited at Santa Cruz station. The quantitative analysis of AOD differences between day and night are shown is table 2, in which we have compared nocturnal and daytime data corresponding to the consecutive 1-h time period during sunrise-moonset (SS-MS) and moonset-sunrise (MS-SR). We can see from these results that differences are $\sim$0.01 in longer wavelength channels and $\sim$0.02 in 500nm and 440nm channels under high illumination conditions (from 86 % in March 12 to 89% in March 20), period of nearly constant aerosol loads. These values are within the AOD accuracy limit established for the standard CE-318 instrument (Holben et al., 1998). From this date on, an increase in the CE-318U inaccuracies at nighttime can be observed (up to 0.03), more importantly in those channel with higher wavelengths (at 1020 nm and 1640 nm). We suspect it can be due to the wavelength dependent inaccuracies affecting to the ROLO model, which seems to become $\leq$0.03 for factor of illumination (FI) $<$80%, being higher at longer wavelengths.

5.2 Precipitable Water Vapor

The comparison of PWV at daytime extracted from AERONET and PWV at nighttime using the CE-318U is displayed in Fig. 2. We have used the same criteria than in the previous AOD comparison to determine quantitatively the day/night discrepancies. This information is presented in table 3. Day and night PWV matches reasonably well in those periods of low PWV temporal variability (from March 12-13 and March 15-21), with discrepancies within the estimated a precision in PWV from sun-photometry $\sim$10% (Holben et al., 2001) as well as the values found by Barreto et al. (2013b). The exception was found in full moon and near full moon events (SS-MR and SR-MS of March 15-16 as well as the SS-MR of March 16), in which the AOD curvature as a result of ROLO inaccuracies lead to higher uncertainties

Table 2: AOD averaged differences extracted from AERONET daytime data and CE-318U nighttime data between during sunset-moonrise (SS-MR, as the last 1-h of daytime data versus the first 1-h of nocturnal data) and moonset-sunrise (MS-SR, as the first 1-h of daytime data versus the last 1-h of nocturnal data). Is included the average moon's fraction of illumination (FI) during nighttime.

	Channel (nm)	1640	1020	870	675	500	440
12-13 Mar. (FI=86%)	SS-MR	0.0115	0.0175	0.0100	0.0078	0.0015	-0.0057
	MS-SR	-0.0025	-0.0016	-0.0024	-0.0066	-0.0092	-0.0098
13-14 Mar. (FI=92%)	SS-MR	-0.0075	-0.0060	-0.0029	-0.0055	-0.0046	-0.0069
	MS-SR	0.0086	0.0080	0.0107	0.0062	0.0064	0.0029
15-16 Mar. (FI=96%)	SS-MR	0.0082	0.0070	0.0107	0.0092	0.0102	0.0071
	MS-SR	− − −	− − −	− − −	− − −	− − −	− − −
16-17 Mar. (Full Moon)	SS-MR	0.0067	0.0069	0.0077	0.0053	0.0066	0.0058
	MS-SR	-0.0072	-0.0086	-0.0081	-0.0117	-0.0135	-0.0162
17-18 Mar. (FI=98%)	SS-MR	-0.0120	-0.0079	-0.0052	-0.0065	-0.0067	-0.0073
	MS-SR	0.0002	0.0027	0.0012	-0.0028	-0.0046	-0.0069
18-19 Mar. (FI=95%)	SS-MR	-0.0046	-0.0048	-0.0051	-0.0080	-0.0093	-0.0111
	MS-SR	-0.0002	-0.0008	0.0023	-0.0018	-0.0014	-0.0053
19-20 Mar. (FI=89%)	SS-MR	-0.0072	-0.0056	-0.0058	-0.0089	-0.0102	-0.0122
	MS-SR	-0.0003	0.0032	0.0039	0.0001	-0.0012	-0.0052
20-21 Mar. (FI=81%)	SS-MR	0.0252	0.0223	0.0216	0.0213	0.0211	0.0182
	MS-SR	0.0105	0.0178	0.0095	0.0075	0.0087	0.0039
21-22 Mar. (FI=71%)	SS-MR	− − −	− − −	− − −	− − −	− − −	− − −
	MS-SR	0.0267	0.0232	0.0160	0.0155	0.0016	0.0005

on PWV. We also attribute the higher than expected discrepancies found in MS-SR of March 13 to calibration problems inherent to ROLO accuracy. Finally, PWV differences > 0.3 found in March 22 MS-SR are attributed to the sparsity of PWV data.

5.3 Synergy with Lidar

5.3.1 Aerosol Mass Concentration

The aerosol mass concentration, whose method was previously presented in Section 4, was processed for the period 2006-2012. Results at ground level (extrapolated from 150 m) and in-situ measurements (PM_{10}) from the TEOM conducted by LISA in this time period are presented in the Fig. 3 (Mortier, 2013). We observe a good correlation between measurements and estimation. The yearly cycles with maximum occuring during winter and minimum during summer are well reproduced. The concentration levels are also similar. In 20% of cases, the difference between estimations and measurements is less than $10\mu g.m^3$. If we consider a difference of $25\mu g.m^3$, which remains coherent regarding high concentration levels on this site, more than 40% of cases are matching (Mortier, 2013).

We present, in Fig. 4a, similar retrievals at daily scale on November 28, 2013. The correlation remains good in this case although the concentration at ground level doesn't highlight strong variations. If the measurements and the method can be validated at ground level, the last can be applied along the whole extinction profile to assess mass concentration vertical profiles (Mortier et al., 2012). Results for this day are presented in the Fig. 4b. The profiles show, in altitude, a stronger time variation, with a maximum of concentration at 13:00 UT between 2 and 3 km height around 150 $\mu g.m^3$. The integration of these profiles can provide the columnar mass concentration whose average is, for this day, about 0.23 $g.m^2$.

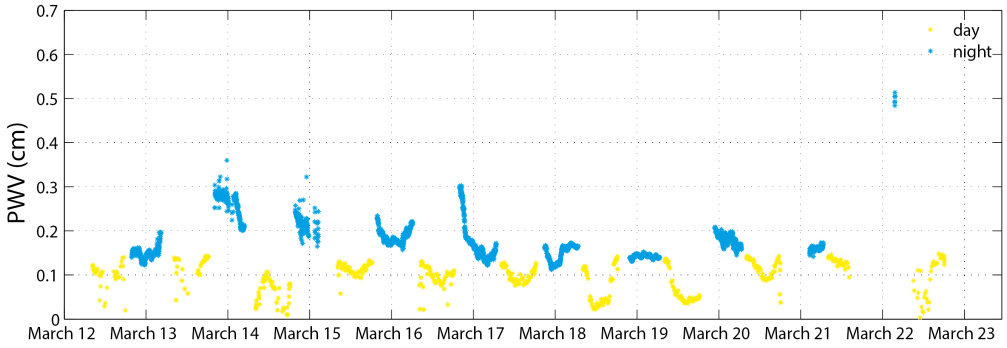

Figure 2: PWV evolution during 10 different days and 9 different nights in March, 2014 using AERONET and CE-318U data at Izaña Observatory.

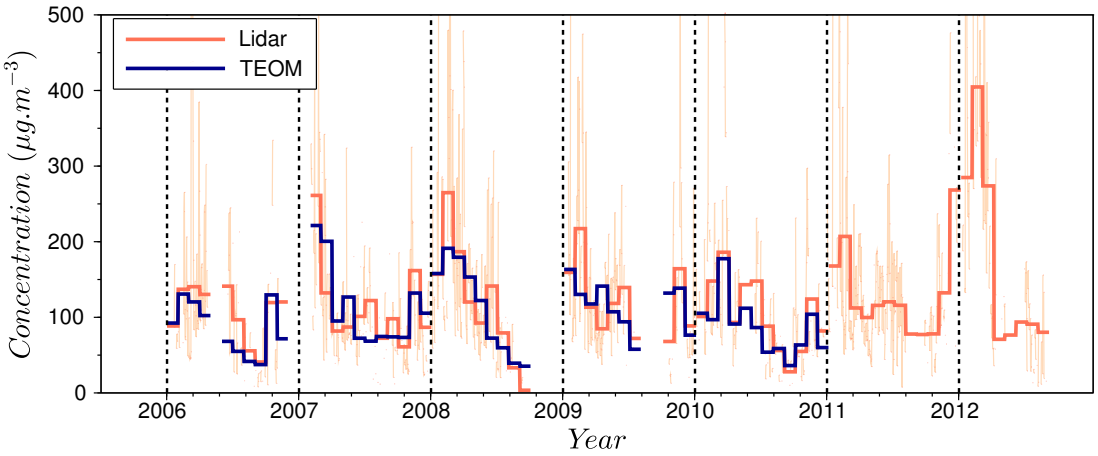

Figure 3: Time series of aerosols mass concentration at ground level at Mbour. In light/dark orange, daily/monthly averages estimations from the lidar-sun-photometer synergy. In blue, in-situ measurements (PM_{10}) performed by a co-located TEOM

5.3.2 Night Inversions

We used the lunar-photometer (CE-318U), in operation at Mbour since 2013, to increases the number of daily AOD measurement for lidar constrained inversions and therefore to retrieve a more accurate extinction vertical profiles at nighttime. We obtained the extinction vertical profiles between two consecutive days (February 12-13, 2014). In the Fig. 5a we present lidar attenuated backscattered profiles for this period. AOD measurements used for inversions and relative calculated extinction profiles, $\sigma_{a,ext}(z)$, and lidar ratio, S_a, are plotted in Fig. 5b. One can notice the progressive increase of AOD between February 12 (0.1) and the end of February 13 (0.50). Extinction coefficients follow this behavior since maximum values, for these two days, are respectively around 0.10 km^{-1} and more than 0.40 km^{-1}. The time dynamic of the atmosphere involve different behaviors for nighttime profiles. Indeed, the boundary layer height is then minimum, and most of aerosols are distributed along the residual layer. These accurate profiles would not be obtained with an inversion constrained by S_a (assumed according to calculated daytime values) because a significant variation of this parameter is observed in the night from February 12 and 13 (50-80 sr), probably due to a change in relative humidity. In that case, assuming the last S_a retrieved daytime (February 12) would result in underestimated extinction profiles up to 40% during

Table 3: PWV differences (cm) extracted from AERONET and CE-318U between daytime and nighttime data during sunset-moonrise (SS-MR, as the last 1-h of daytime data versus the first 1-h of nocturnal data) and moonset-sunrise (MS-SR, as the first 1-h of daytime data versus the last 1-h of nocturnal data)..

		PWV difference (cm)
12-13 Mar. (FI=86%)	SS-MR	-0.0174
	MS-SR	0.0558
13-14 Mar. (FI=92%)	SS-MR	-0.1404
	MS-SR	-0.1670
14-15 Mar. (FI=96%)	SS-MR	-0.1766
	MS-SR	-0.0856
15-16 Mar. (Full Moon)	SS-MR	0.0787
	MS-SR	-0.1078
16-17 Mar. (FI=98%)	SS-MR	0.1818
	MS-SR	0.0317
17-18 Mar. (FI=95%)	SS-MR	0.0420
	MS-SR	-0.0497
18-19 Mar. (FI=89%)	SS-MR	-0.0020
	MS-SR	-0.0083
19-20 Mar. (FI=81%)	SS-MR	− − −
	MS-SR	-0.0143
20-21 Mar. (FI=71%)	SS-MR	-0.0269
	MS-SR	-0.0090
21-22 Mar. (FI=71%)	SS-MR	− − −
	MS-SR	-0.3228

nighttime.

6 THE NEW SUN/MOON/SKY PHOTOMETER CE-318T

Since the new CE-318T will certainly serve to enhance the aerosol characterization through its capability to perform a complete cycle of diurnal photometric measurements at both day and nighttime, we introduce a brief description of this instrument in this Section. This new photometer, recently developed by Cimel Electronique, combines the features of the extensively used CE-318 with the ability to perform nocturnal measurements of the CE-318U. It has the triple function of performing spectral direct sun, direct moon measurements of aerosol and water vapor concentrations in addition to daytime spectral sky radiances to infer aerosol properties from inversion. It was installed at Izaña Observatory on 2014. We can see in Fig. 6 the AOD and PWV evolution, respectively, extracted from day and night CE-318T measurements in the period from March 12 to March 23. Our results suggest (not showed) a good agreement between CE-318T daytime and AERONET data in addition to an apparent daily sequence of AOD and PWV measurements.

Future thorough studies will be developed to completely assess the instrument performance as well as to check the ability improvement of the combined lidar/photometer observation system using this new device. In addition, the new features of this instrument permit to be calibrated by transference from a master at both day and nighttime using the only diurnal measurements, which allows us to reduce the complexities inherent to nocturnal calibration due to the low signal captured at nighttime.

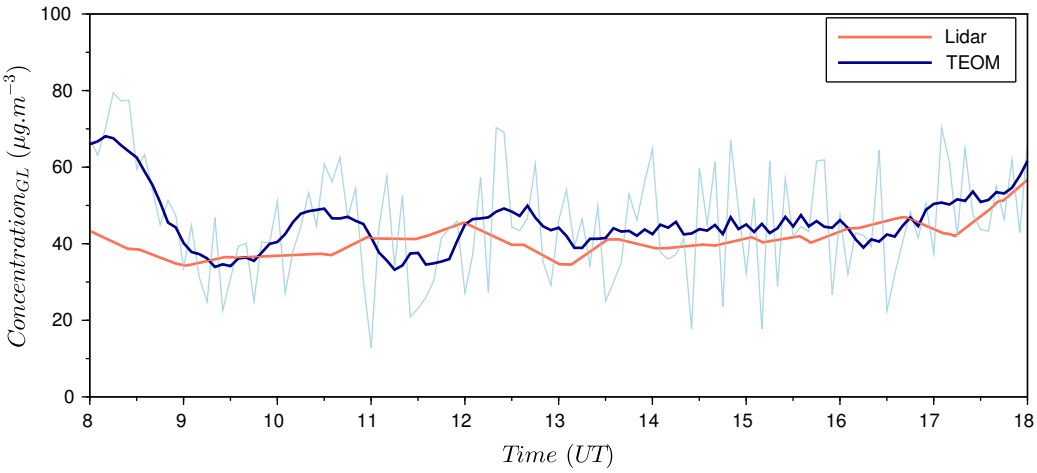

(a) In orange/blue, estimation/measurements of mass concentration at ground level

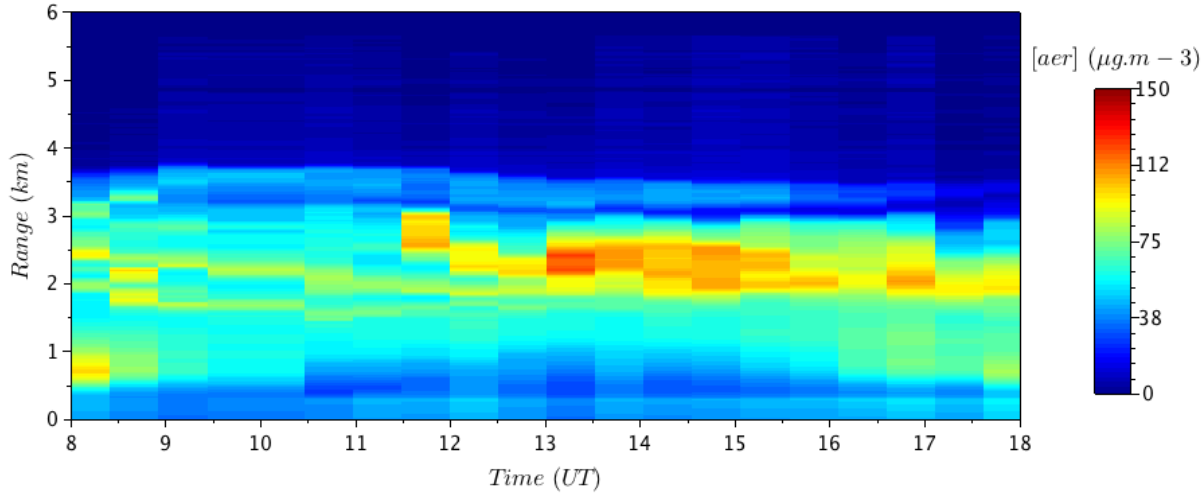

(b) Mass concentration profiles estimated from lidar and sun-photometer synergie

Figure 4: Mbour mass concentration measurements carried out on November 28, 2013

7 SUMMARY AND CONCLUSIONS

In this paper we have described the lunar-photometer CE-318U, designed to perform nocturnal photometric measurements with a moon as a light source and assessed the instrument's performance by means of a comparative analysis of nocturnal (CE-318U) and daytime AERONET AOD and PWV. We derived AOD and PWV in a 10 days and 9 nights period in March, 2014, at the high mountain Izaña Observatory. The AOD comparative study reported discrepancies similar to the sunphotometry precision in the AERONET network ($\pm$0.01-0.02) for those periods not affected by significant aerosol concentration variability and high moon illumination conditions (up to $\sim$ 85%). However, lower accuracy is expected under lower FI cases ($\geq$ 0.03), being these errors higher at longer wavelength channels due to ROLO inaccuracies. In addition, these uncertainties at low FI cases are consequently attributed to the expected decrease in signal-to-noise ratio. In case of PWV, the comparison showed that PWV at daytime and nighttime matched reasonably well in those conditions of a expected stability in this atmospheric constituent, with discrepancies within the estimated precision of $\sim$ 10% predicted by Holben et al. (1998). Some exceptions to this good performance were also found as a result of uncertainties in the ROLO implemented model as well as the effect of the reduced energy at low illumination conditions.

The synergetic retrieval of AOD at nighttime from the combined lidar/lunar-photometer system was

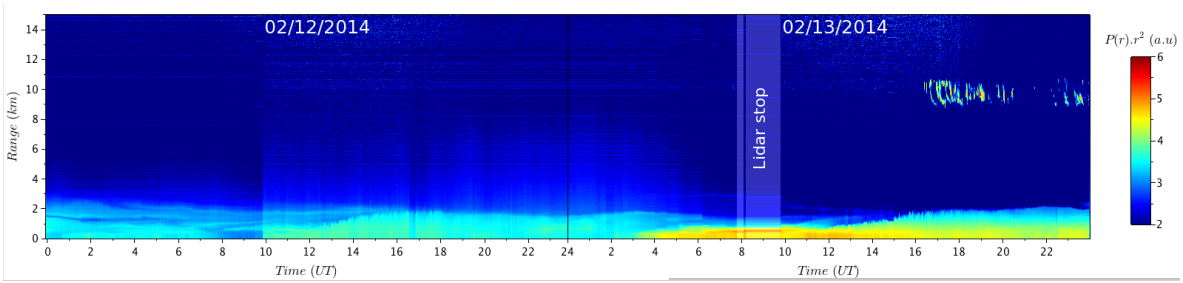

(a) Attenuated backscattered profiles

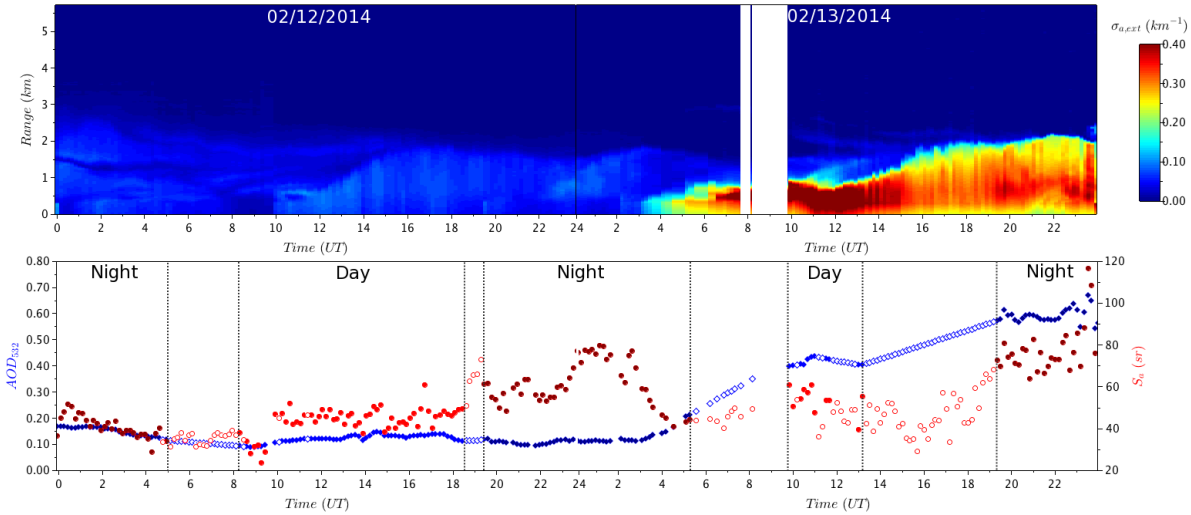

(b) On top, extinction profiles. On the bottom, in light/dark blue filled diamonds, daytime/nighttime AOD. The red circles are respective values of S_a. Empty symbols correspond to inversions realized with interpolated AOD.

Figure 5: Mbour attenuated backscatter and extinction profiles during two consecutive days (Febrary 12-13, 2014) and AOD retrieval.

checked using the CE-318U instrument deployed at Mbour (West Africa). It has led us to a more accurate extinction vertical profile calculation at nighttime than the profile obtained with an inversion constrained by the daytime S_a value. In our case study, the assumption of S_a to perform lidar inversion would result in a underestimated extinction profile up to 40% at nighttime, probably due to changes in the relative humidity not considered using only day information.

Finally, we have briefly introduced the new photometer CE-318T, capable to perform a complete cycle of diurnal photometric measurements at both day and nighttime. The new improvements of this new device permit this new photometer version to extend photometric information at nighttime using the moon as a light source as well as to reduce the complexities inherent to nocturnal calibration due to the low signal captured at nighttime.

To conclude, we have demonstrated with this paper the capability of the CE-318U for aerosols and atmospheric water vapor monitoring and the enhancement in the aerosol characterization by means of the synergy of the combined lidar/lunar-photometer observation system. Furthermore, these abilities can be extended using the new instrument CE-318T, recently developed to perform direct sun, direct moon and sky spectral measurements.

8 acknowledgements

This work was supported by AERONET-EUROPE (European Communitys FP7-INFRASTRUCTURES-2010-1 under grant agreement no. 262254-ACTRIS). The authors thank the AERONET team for making

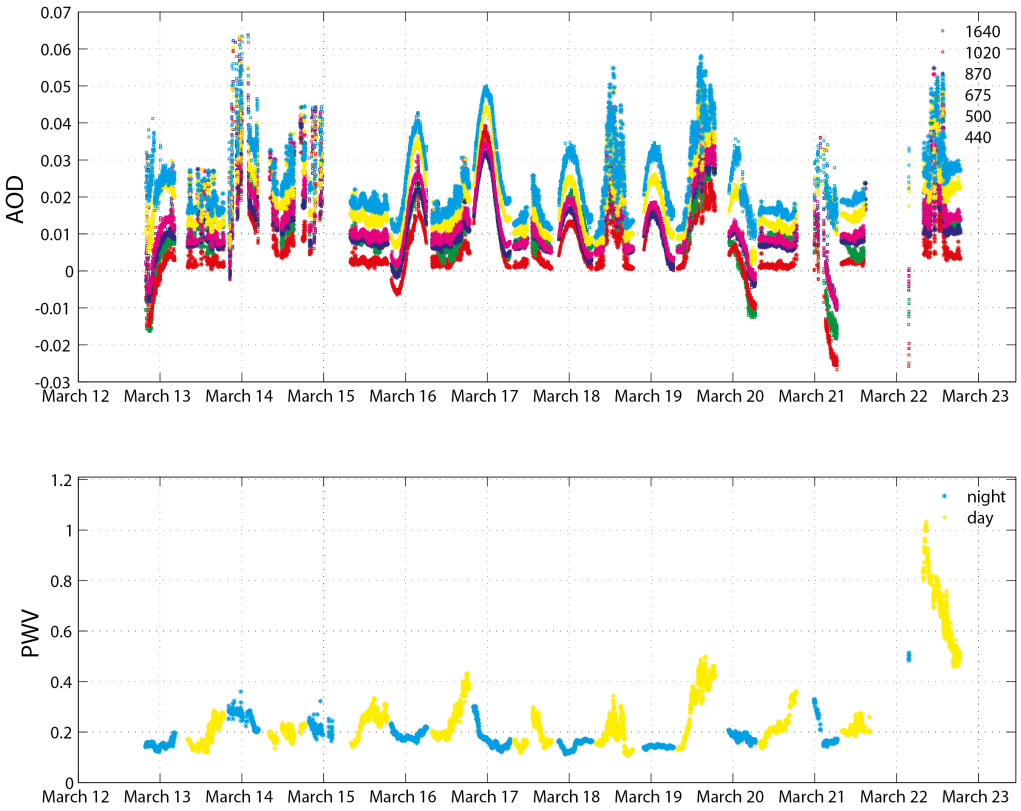

Figure 6: AOD (upper panel) and PWV (lower panel) evolution during 10 different days and 9 different nights in March, 2014, using the new CE-318T data at Izaña Observatory.

data available.

References

Barreto, A., Cuevas, E., Damiri, B., Guirado, C., Berkoff, T., Berjón, A. J., Hernández, Y., Almansa, F., and Gil, M.: A new method for nocturnal aerosol measurements with a lunar-photometer prototype, Atmos. Meas. Tech. 6, 585-598, doi:10.5194/amt-6-585-2013, 2013.

Barreto, A., Cuevas, E., Damiri, B., Romero, P. M., and Almansa, F.: Column water vapor determination in nigth period with a lunar-photometer prototype, Atmos. Meas. Tech., 6, 2159-2167, doi:10.5194/amt-6-2159-2013, 2013.

Bruegge, C. J., Conel, J. E., Green, R. O., Margolis, J. S., Holm, R. G., and Toon, G.: Water vapor column abundances retrievals during FIFE, J. Geophys. Res., 97, 18759-18768, 1992.

Chaikovsky, A., Bril A., Dubovik O., Holben B, Thompson A., Goloub P., ONeill N., Sobolewski P., Bsenberg J, Ansmann A., Wandinger U., Mattis I. CIMEL and multiwavelength lidar measurements for troposphere aerosol altitude distributions investigation, long-range transfer monitoring and regional ecological problems solution: field validation of retrieval techniques, Òptica Pura y Aplicada. 37(3). P. 3241-3246, 2004.

Chaikovsky, A.P., Denisov, S.V., Grudo, Ya.O., Lopatsin, A.Yu, Koro,l M.M., Osipenko, F.P., Savitski, D.A., Slesar, A.S., Chaikovskaya, L.I., Dubovik, O., Goloub, P., Tanrè, D., Lapyonok, T., and Korol, Y.: Combined lidar and radiometric sounding of atmospheric aerosol: algorithm of data processing,

software, dessimination in: "Proceedings of XVIII International symposium "Atmospheric and ocean optics. Atmosphere physics", 2-6 Jult, 2012, Irkutsk, Russian Federation, C1-C4, 2012.

Chaikovsky, A., Dubovik, O., Goloub, P., Tanrè, D., Pappalardo, G.,Wandinger, U., Chaikovskaya, L., Denisov, S., Grudo, Y., Lopatsin, A., Karol, J., Lapyonok, T., Korol, M., Osipenko, F., Savitski, D., Slesar, A., Apituley, A., Alados Arboledas, L., Binietoglou, I., Kokkalis, P., Granados Munoz, M. J., Papayannis, A., Perrone, M. R., Pietruczuk, A., Pisani, G., Rocadenbosch, F., Sicard, M., De Tomasi, F., Wagner, J., and Wang, X.: Algorithm and software for the retrieval of vertical aerosol properties using combined lidar/radiometer data: dissemination in EARLINET, Reviewed Revised Papers of the 26th International Laser Radar Conference, 2529 June, Porto Heli, Greece, Paper SO3-09, 2012.

Cuesta, J., Flamant, H. P., and Flamant, C.: Synergetic technique combining elastic backscatter lidar data and sun-photometer AERONET inversion for retrieval by layer of aerosol optical and microphysical properties, Appl. Optics, 47, 4598-4611, 2008.

Fernald, F. G.: Analysis of atmospheric lidar observations Some comments, Appl. Optics, 23, 652-653, 1984.

Halthore, R. N., Eck, T. F., Holben, B. N., and Markham, B. L.:Sun photometric measurements of atmospheric water vapor column abundance in the 940-nm band, J. Geophys. Res., 102, D4, 4343-4352, 1997.

Holben, B. N., Eck, T. F., Slutsker, I., Tanrè, D., Buis, J. P., Setzer, A., Vermote, E., Reagan, J. A., Kaufman, Y. J., Nakajima, T., Lavenu, F., Jankowiak, I. And Smirnov A.: AERONET- A federated instrument network and data archive for aerosol characterization, Rem. Sens. Environ., 66, 1-16, 1998.

Holben, B. N, Tanré, D., Smirnov, A., Eck, T. F., Slutsker, I., Abuhassan, N., Newcomb, W. W., et al.: An emerging ground-based aerosol climatology: Aerosol Optical Depth from AERONET, Journal of Geophysical Research, Atmospheres (1984-2012), 106, D11, 12067-12097, DOI: 10.1029/2001JD900014, 2001.

Kieffer, H. H., and Stone, T. C.: The spectral irradiance of the moon, The Astronomical Journal, 129, 2887-2901, 2005.

Klett, J.D.:Inversion with variable backscatter/extinction ratios. Appl. Optics 11, 1638-1643, 1985.

Léon, J. F., Derimian, Y., Chiapello, I., Tanr, D., Podvin, T., Chatenet, B., and Deroo, C. (2009). Aerosol vertical distribution and optical properties over M'Bour (16.96 W; 14.39 N), Senegal from 2006 to 2008. Atmospheric Chemistry and Physics, 9(23), 9249-9261.

Lopatin, A., Dubovik, O., Chaikovsky, A., Goloub, P., Lapyonok, T., Tanrè, D., and Litvinov, P.: Enhancement of aerosol characterization using synergy of lidar and sun-photometer coincident observations: the GARRLiC algorithm, Atmos. Meas. Tech., 6, 20652088, doi:10.5194/amt-6-2065-2013, 2013.

Mortier, A., Goloub, P., Podvin, T., Deroo, C., Chaikovsky, A., Ajtai, N., Blarel, L., Tanre, D., and Derimian, Y.: Detection and characterization of volcanic ash plumes over Lille during the Eyjafjallajökull eruption, Atmos. Chem. Phys. Discuss., 12, 3103131070, doi:10.5194/acpd-12-31031-2012, 2012.

Mortier. A., Tendances et variabilités de l'aérosol atmosphérique à l'aide du couplage Lidar/Photomètre sur les sites de Lille et Dakar, Phd Thesis, Laboratoire dOptique Atmosphérique, U.F.R de Physique, Université Lille 1, Sciences et Technologies, 59655 Villeneuve dAscq, France, University of Lille, Decembre 2013.

J. Pelon, M. Mallet, A. Mariscal, P. Goloub, D. Tanr, D. Bou Karam, C. Flamant, J. Haywood, B. Pospichal, and S. Victori. (2008). Microlidar observations of biomass burning aerosol over Djougou

(Benin) during African Monsoon Multidisciplinary Analysis Special Observation Period 0: Dust and Biomass Burning Experiment. Journal of Geophysical Research: Atmospheres (19842012), 113(D23).

Perrone, M. R., De Tomasi, F., and Gobbi, G. P.: Vertically resolved aerosol properties by multi-wavelength lidar measurements, Atmos. Chem. Phys., 14, 11851204, doi:10.5194/acp-14-1185-2014, 2014.

Schmid, B., Thome, K. J., Demoulin, P., Peter, R., Mätzler, C., and Sekler, J.: Comparison of modeled and empirical approaches for retrieving columnar water vapor from solar transmittance measurements in the 0.94-m region, J. Geophys. Res., 101, D5, 9345-9358, 1996.